Brandon Roman

Mid-Infrared Complex Refractive Indices for Motor Oil

Spring Quarter, 2017

Thesis submitted in completion of Honors Senior Capstone requirements for the
DePaul University Honors Program

Dr. Richard Niedziela, Department of Chemistry
Dr. Graham Griffin, Department of Chemistry

Table of Contents

MID-INFRARED COMPLEX REFRACTIVE INDICES FOR MOTOR OIL

Brandon Roman, Stephanie E. Goyette, Daniel J. Olesak, Richard F. Niedziela, Ph.D.
Department of Chemistry, DePaul University, Chicago IL, United States

ABSTRACT

Given their potential impact on the environment, aerosols and their properties are of keen scientific interest. One class of these aerosols are those related to internal combustion processes. In this case, motor oil particles formed in large quantities may have a significant effect on local environments. To aid in the assessment of the environmental impact of these particles, frequency-dependent, complex refractive indices for Pennzoil 5W-20 motor oil were retrieved directly from aerosol extinction spectroscopy between 700 cm^{-1} and 5000 cm^{-1}. Complex refractive indices allow one to predict how an aerosol scatters and absorbs light. These basic data can be used in applications such as particle sizing and chemical speciation, both of which can help elucidate the impact of motor oil droplets on the atmosphere.

INTRODUCTION

Atmospheric aerosols are linked to significant impacts on climate, human health, air quality, cloud formation, and visibility. One such type of particle that can affect the latter three areas may be motor oil droplets that are sourced from internal combustion engines. This aerosolized form of motor oil can contribute directly to environmental effects (e.g., reduction of visibility), or via indirect mechanisms (**Figure 1**). Motor oil droplets can serve as a substrate for surface-based reactions involving other species. This can result in the generation of secondary aerosols that can further impact the environment. The full environmental effect of these small particles cannot be determined at this time due to incomplete knowledge about their chemical,

optical, and physical properties, as well as their complex spatial and temporal distributions throughout the atmosphere.

Motor oil aerosols are mixtures of many organic compounds, the composition of which ultimately determines their chemical and physical properties. This project focuses on the determination of complex refractive indices for motor oil using Fourier Transform Infrared (FT-IR) spectroscopy. Complex refractive indices, or optical constants, determine how a material absorbs and scatters light as a function of frequency. These data can be used by other investigators to determine the size, composition, and other characteristics of aerosolized motor oil in the field using simple spectroscopic methods.

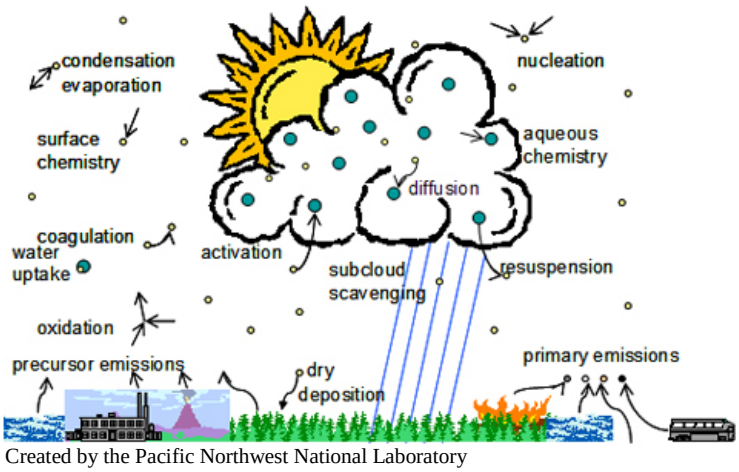

Created by the Pacific Northwest National Laboratory

<u>Figure 1:</u> Available Pathways for Aerosol Emission. Diagram illustrating the multiple pathways that a primary aerosol can undertake after emission. The number processes available to motor oil aerosols make its environmental effects difficult to study.

Using spectroscopic methods, it is important to note that the extinction of light by an aerosol is governed not only by particle size, but also by its shape and number density. The extinction is also dependent upon the frequency of the light, $\tilde{\nu}$, (units of wavenumber, cm^{-1}),

through the complex refractive indices, *N*, of the material from which the aerosol is made. Equation 1, given below, shows the dependence that the complex refractive index has on its real (*n*) and imaginary (*k*) components.

$$N = n(\tilde{\nu}) + i\kappa(\tilde{\nu}) \qquad (\mathbf{1})$$

The real component governs photon scattering, while the imaginary component is responsible for photon absorption. Three basic types of scattering exist: Rayleigh, geometric, and Mie scattering. Rayleigh scattering deals with objects that are smaller than the incoming wavelength. Rayleigh scattering has a strong wavelength dependence and the scattering increases linearly as the size increases. Geometric scattering describes scattering when the object interacting with light is much larger than the wavelength. In Mie scattering, the wavelength of the incoming light is similar to the size of the interacting particle, which for the lab-generated aerosols in this study is around the order of microns. Therefore, using a Mie inversion method (elaborated upon in the experimental section), the complex refractive indices for motor oil can be found.

Past research involving infrared red (IR) analysis of combustion engine emissions has been carried out by others. Similar to this project, a geophysical research group analyzed on-road gasoline and diesel-powered vehicle emissions in Nashville, Tennessee.[1] The study quantified on-road vehicle emissions of carbon monoxide (CO), non-methane hydrocarbons (NMHC), and oxides of nitrogen (NO_x) by IR spectroscopy. Strikingly, the group found that approximately 50% of NO_x emissions overall originated from on-road vehicles while those of CO and NMHC were found to be insignificant.

A different group also employed Fourier-Transform infrared (FT-IR) spectroscopy coupled to cluster analysis chemometrics in their investigation of high quality motor oil adulteration (the mixing of high quality oils with inferior varieties). The aim of the research was to develop a partial

least squares model to predict adulteration within a concentration range of 0-36% (w/w). From the ranges of 1800-600 cm^{-1}, the group managed to predict adulteration with good accuracy.[2]

Lastly, in a study differentiating motor oils for criminalistics, a group examined sixteen kinds of mineral, synthetic and semi-synthetic motor oils using FTIR spectroscopy. It was found that differentiation of motor oil brands between various oil samples collected in a crime scene could be performed using IR spectroscopy, however other means including X-ray spectroscopy and atomic absorption spectrometry should also be utilized.[3] These studies clearly demonstrate the utility of infrared spectroscopy in elucidating the composition of motor oils.

In this study, the refractive indices will be reported for use in other studies that are designed to assess the impact of motor oil aerosols it in the atmosphere. The ability to identify the different compounds that make up motor oil is of great importance, particularly in identifying compounds that can adversely affect health. Because infrared spectroscopy can be used to "fingerprint" organic compounds, FT-IR spectroscopy can be used to analyze functional groups that exist in motor oil aerosols. Altogether, the ability to examine different functional groups in this manner can provide insight on the impact of motor oil pollution on the environment.

EXPERIMENTAL / CALCULATIONS

As part of the retrieval process, the temperature dependence of the real refractive index at the sodium D-line (589.3 nm), n_D, for Pennzoil 5W-20 motor oil was measured using an Abbe refractometer (Reichert Arias 500). A third order polynomial fit was applied to three independent data sets containing real refractive indices measured at different temperatures (~4 – 45 °C). All temperatures were recorded within ± 0.01 °C. An F-test was also done at the 95% confidence level to support use of a third order polynomial fit. The real refractive index data fitted with a polynomial

curve in order to extract the real refractive index value at 25 ^{o}C to high certainty. (**Figure 2**). The equation of the polynomial fit from figure 2 is:

$n_D(T) = (1.4771 \pm 0.0001) - ((2.3 \pm 0.2) \times 10^{-4})T \cdot (^{o}C^{-1}) - ((5.4 \pm 0.7) \times 10^{-6})T^2 \cdot (^{o}C^{-2}) + ((6.6 \pm 0.9) \times 10^{-8})T^3 \cdot (^{o}C^{-3})$.

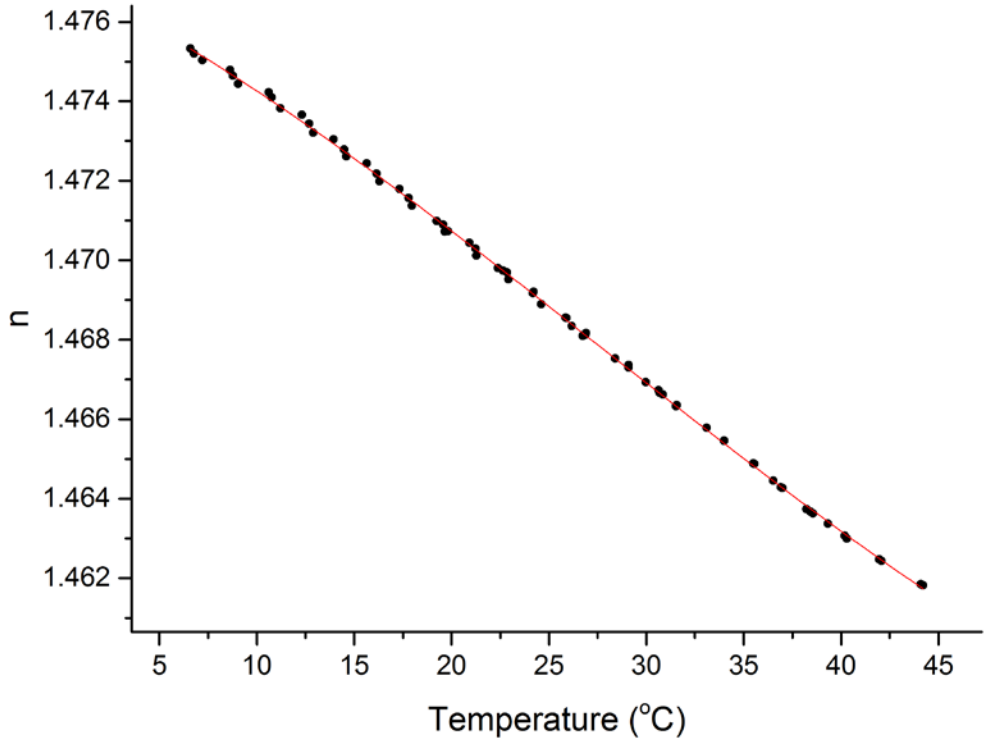

Figure 2: Real Refractive Temperature Dependence. The above figure plots the temperature dependence of the real refractive index for Pennzoil 5W-20 motor oil. The linear regression fit (red line) applied to the refractive index plotted against temperature yielded:

Aerosol extinction spectra were collected using a laminar flow cell enclosed in an acrylic vacuum jacket (**Figure 3**).

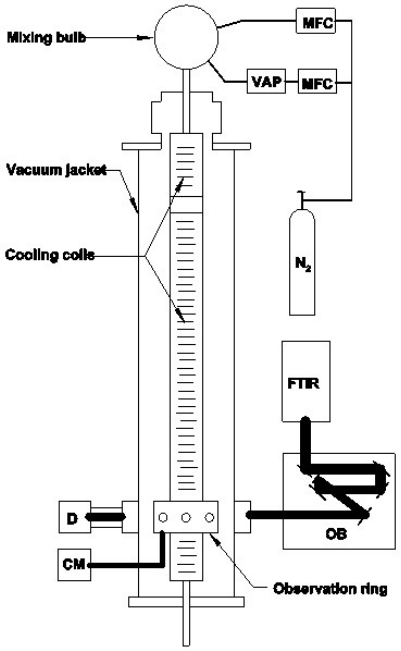

Figure 3: Aerosol Flow Cell Schematic Diagram. The cell is made from three sections of copper tubing (diameter = 7.64 cm), each temperature-controlled by a recirculating chiller. Pennzoil 5W-20 motor oil aerosols are generated (VAP) and injected at the top of the cell. Mass flow controllers (MFC) channeling nitrogen gas are regulated to adjust the number density and size of aerosol particles. As aerosol flows through the observation ring they eventually are probed by the beam emitted from the MB-104 FT-IR spectrometer (FTIR) optic box (OB). The MCT detector (D) is used for IR light detection, while the capacitance monometer (CM) provides the cell pressure.

The motor oil aerosol was generated by homogenous nucleation in a glass vaporizer (**Figure 4**). A regulated stream of nitrogen was channeled through the vaporizer carrying heated motor oil vapor to a cooler region where it condensed into an aerosol. Temperatures of generated aerosol never exceeded 350 ^{o}C to avoid possible decarboxylation of oxygen-containing compounds in the oil. The aerosol extinction spectra were recorded over a range from 700 cm^{-1} to 5000 cm^{-1} by a Bomem MB-104 benchtop FT-IR spectrometer at a resolution of 2 cm^{-1}. Thin-film spectra of liquid phase motor oil, recorded on the same spectrometer, were used to initialize the refractive index retrievals.

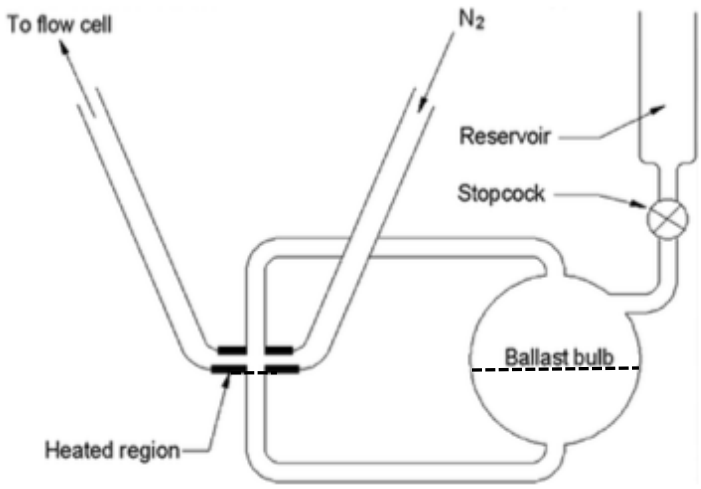

Figure 4: Vaporizer Schematic Diagram. The vaporizer used to generate motor oil aerosol is constructed from borosilicate glass. A resistive heat tape is wrapped around the bottom of the vaporizer with the temperature being controlled by a variable autotransformer. The black dotted line represents an approximate fluid level required for generation of motor oil.

The mid-infrared, frequency-dependent complex refractive indices for motor oil were retrieved via Mie inversion of the aerosol extinction spectra recorded at 25 °C.[4] Similar to previous studies conducted by the Niedziela lab, the inversion method used here utilizes aerosol extinction spectra (*E*) that were collected in the laboratory by measuring the incoming radiant light, *I*, as it interacts with a group of particles. As shown by the Beer-Lambert law, both the aerosol scattering (a_{sca}) and absorption (a_{abs}) of light leads to an overall reduction in irradiance with respect to its initial value (I_o). Equation 2, given below, describing this phenomena and also shows the dependence of aerosol path length as light travels through.

$$E(v) = -\ln\left(\frac{I}{I_0}\right) = \left(a_{abs}(v) + a_{sca}(v)\right)L \qquad (\mathbf{2})$$

Specifically, the Mie inversion procedure of Dohm *et al.* was applied to the collected motor oil aerosol extinction.[4] A non-scattering, thin-film absorption spectrum of motor oil was used to initiate the inversion procedure by providing an estimate of the imaginary component that can be

later scaled.[5] Subsequently, the Kramers-Kronig relationship (given in equation 3 below) was used to provide corresponding frequency-dependent values for the real index component.

$$n(\tilde{\nu}_i) = n(\infty) + \frac{2}{\pi} P \int_0^{\infty} \frac{\tilde{\nu} k(\tilde{\nu})}{(\tilde{\nu}^2 - \tilde{\nu}_i^2)} d\tilde{\nu} \qquad (\mathbf{3})$$

In the equation above, the real component at infinite frequency ($n(\infty)$) and the Cauchy principal value (P) are included in the calculation of the real index component values.[5] Simply, the Cauchy principal value allows for the improper integral to be transformed into a solvable integral. After this step a Mie scattering calculation was carried out using the real and imaginary components around their frequency range of 700 cm^{-1} to 5000 cm^{-1}. It should be noted that the calculation assumes a log-normal particle size distribution (given in equation 4). The particle radius (r), the geometric mean radius (r_g), and the width of the log-normal distribution (σ_g) are also taken into account in the Mie scattering calculation.[5]

$$P_{LN}(r; r_g; \sigma_g) = \frac{1}{r ln(\sigma_g)\sqrt{2\pi}} \exp\left[-\frac{1}{2} \left(\frac{\ln\left(\frac{r}{r_g}\right)}{ln(\sigma_g)} \right)^2 \right] \quad \mathbf{(4)}$$

The resulting spectrum and the collected motor oil aerosol extinction spectrum were then compared to each other to find any discrepancies that could be minimized with a better estimate of the imaginary component. Iterative changes in r_g and σ were also done until convergence occurred between calculated and experimental spectra. It should be noted that Brent's PRAXIS procedure was used to minimize the differences between the calculated and experimental spectra.[5] It is also important to note that most of the experimental spectra were subject to a correction to remove residual water vapor signals. This correction removed any detectable water contamination from the observed motor oil aerosol spectra. A similar CO_2 correction may be applied to fits in the

future as minute traces of it appear in some of the collected spectra. The total process described above is summarized in the flowchart below (**Figure 5**).

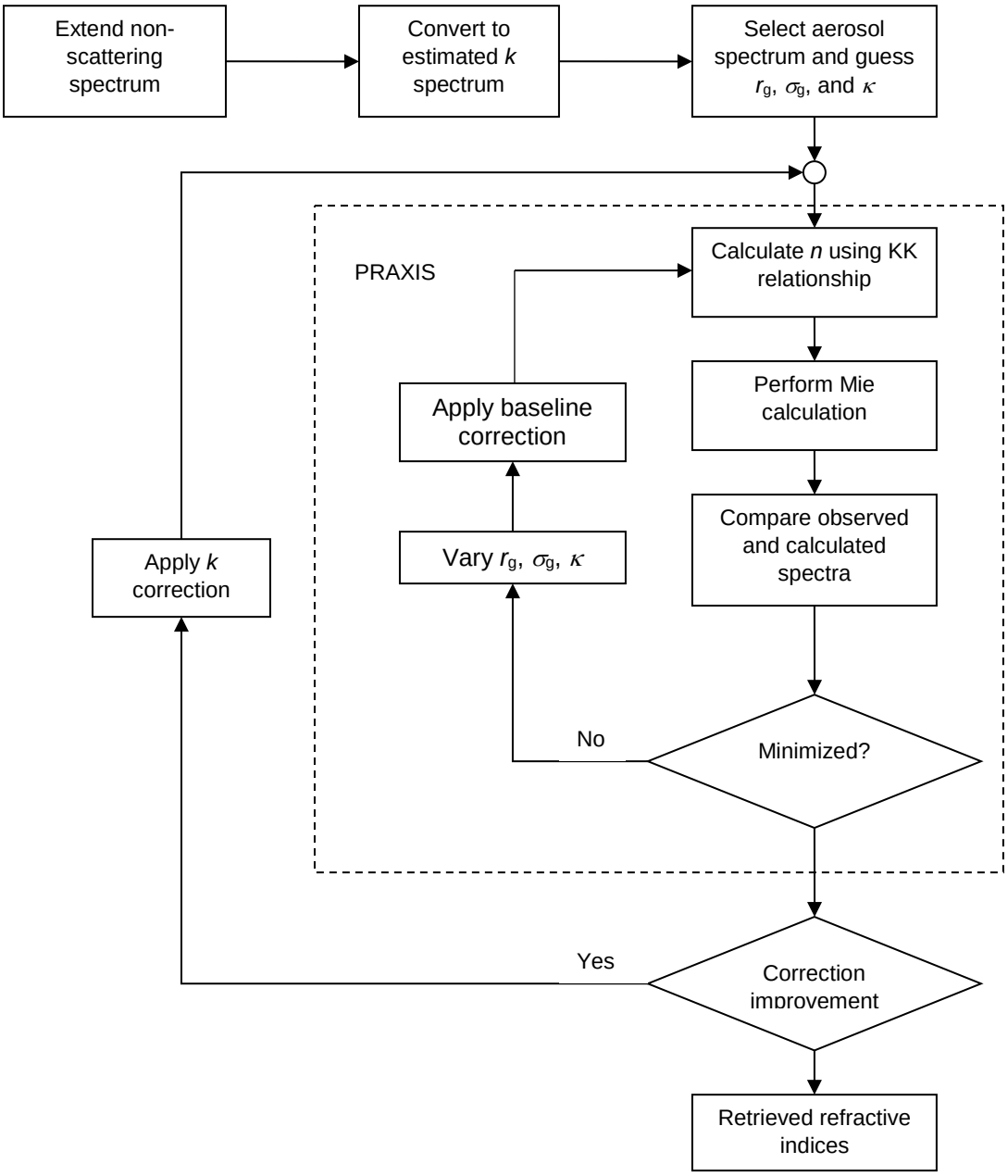

Figure 5: Complex Refractive Index Retrieval Process Flowchart. The dashed box in this diagram encloses the computation operations that are executed in each PRAXIS iteration. Iterations continue until reductions in chi-squared fall below 5%.

RESULTS AND DISCUSSION

The complex refractive indices for 30 generated motor oil aerosols were retrieved as described previously. The thin-film spectrum utilized for the retrieval process is provided below with key regions of interest magnified (**Figure 6**). There are a variety small stretches occurring in the low wavenumber range not seen at the higher wavenumber region.

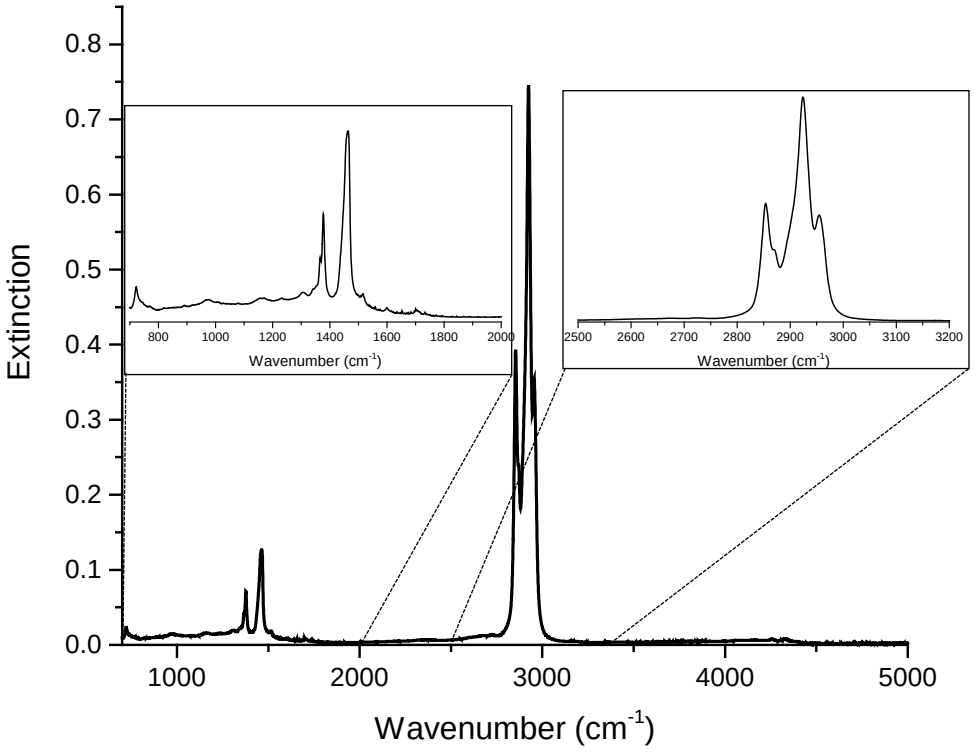

<u>Figure 6</u>: Motor Oil Thin-Film Spectrum. The thin-film spectrum for liquid-phase motor oil is given with key regions magnified to show less prevalent stretches observed within the mid-infrared. Significant IR stretches are seen occurring around 2800-3000 cm^{-1} and 1300-1500 cm^{-1} regions.

A few experimental spectra that later underwent the fitting process using the above thin-film spectrum are provided below (**Figure 7**). It should be noted that the spectra have been offset

from each other for better clarity and comparison. The different baseline curvature and band intensities are the expected result of varying flow, temperature, and cell pressure conditions. Larger curvatures at the high wavenumber range correspond to larger aerosol particles which scatter light more than smaller particle distributions.

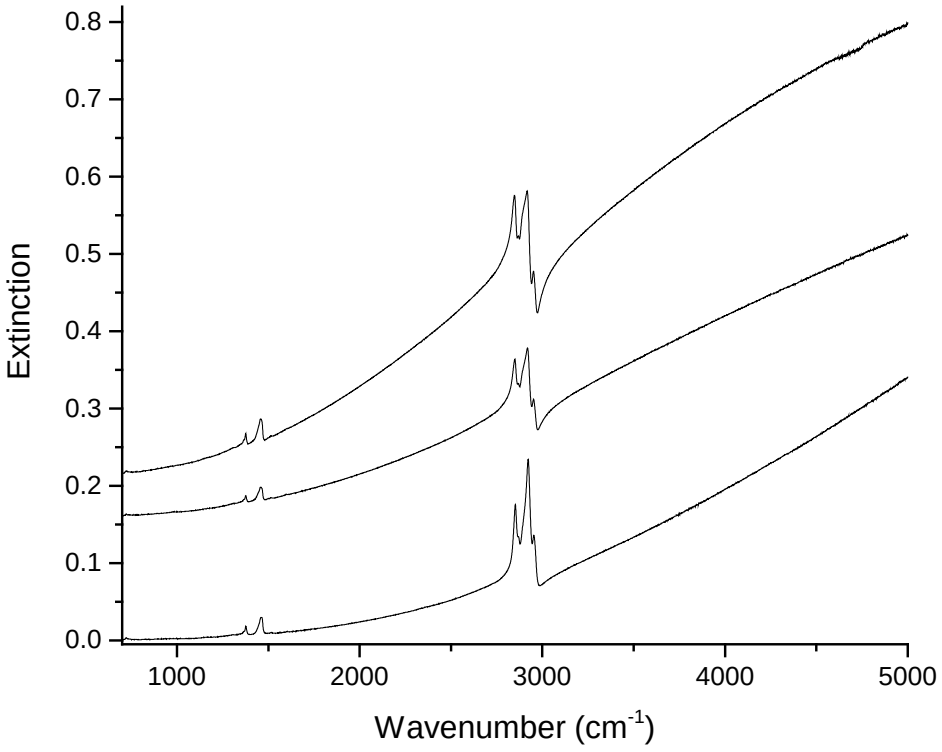

Figure 7: Three Example Motor Oil Aerosol Spectra. Shown above are three of the 30 motor oil spectra used in the complex refractive index retrieval process. The spectra have been purposely offset for better comparison. The upward sloping base line a result of the aerosol scattering component. Different cell pressures, flows, and temperature conditions used in the generation of the aerosol have a significant influence on the curvature and band intensities.

The example spectra above, along with 27 other collected extinction spectra, were subjected to the Mie inversion retrieval process. One example extinction spectrum overlaid with the resulting fit is given below (**Figure 8**). Overall, there seems to be little discrepancy in all mid-

range wavenumber regions. The highest discrepancy is only observed toward the high wavenumber end of the spectra due to unavoidable noise in each experimental spectrum. Interestingly, a carbon dioxide band seems to be present in some of the spectra collected since a small uncertainty can be seen at 2400 cm^{-1}.

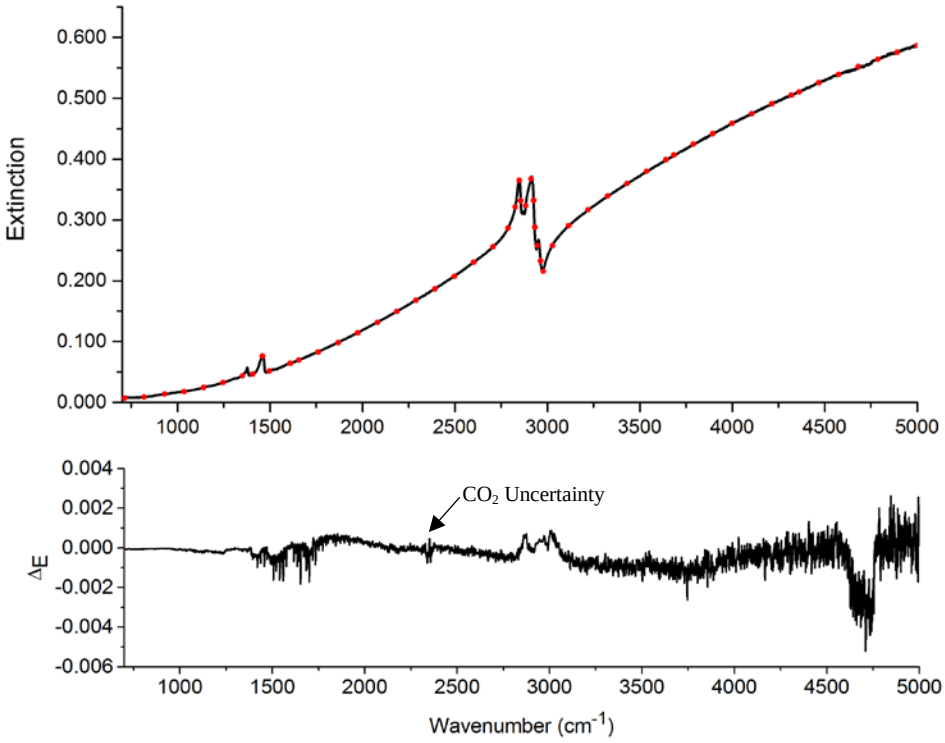

Figure 8: Motor Oil Example Retrieval Result. An example retrieval result is given for motor oil with associated error between the experimental and calculated spectra. The top panel contains the experimental aerosol spectrum (solid black line) overlaid with the results of the Mie calculation (red dotted line). The bottom panel shows the discrepancies associated between the two spectra.

Finally, all found refractive index sets were averaged to produce the final set of data (**Figures 9 and 10**). Specifically, Figure 9 shows the imaginary component spectrum for motor oil

which again shows little error in the mid-wavenumber regions. The maximum k value was found to be 0.1792 occurring at 2923.87 cm^{-1}.

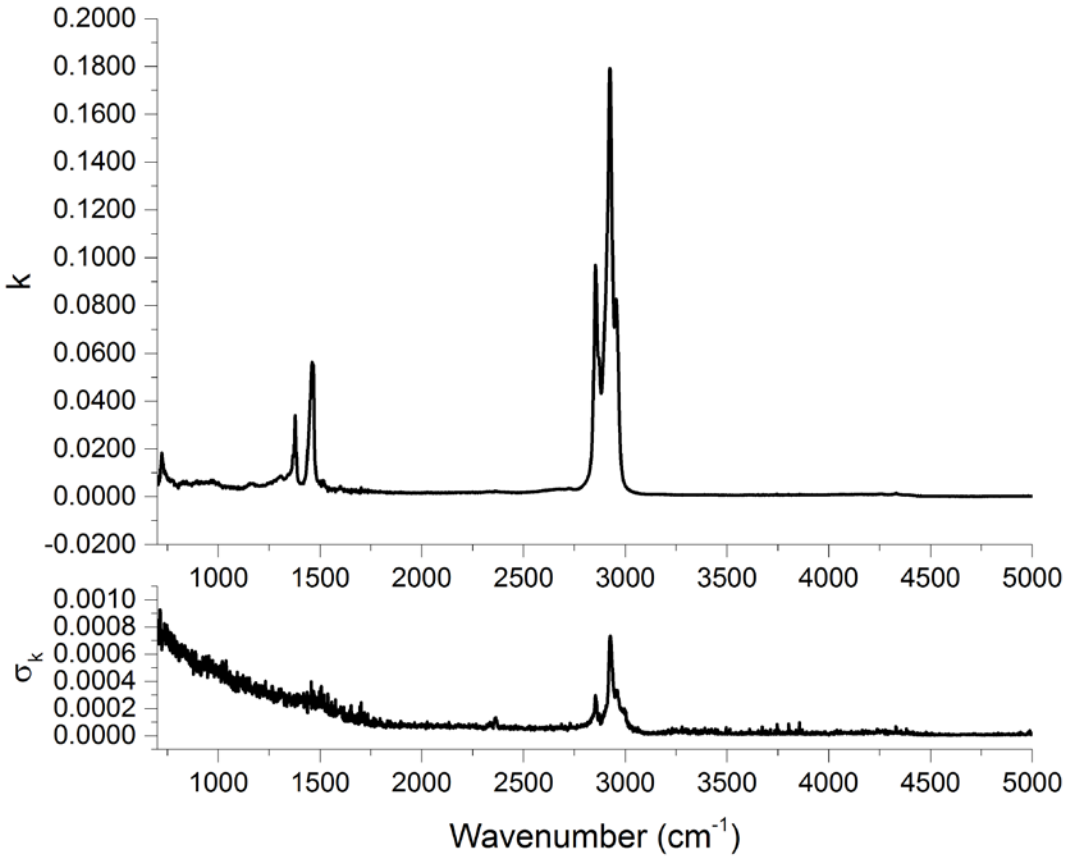

<u>Figure 9:</u> Imaginary Component Spectrum. The top panel provides the imaginary component spectrum for motor oil after subjecting 30 experimental spectra to the Mie retrieval process. The lower panel shows the error associated in the spectrum with a small peak of approximately 2400 cm^{-1} appearing for CO_2 uncertainty.

Figure 10 plots the real component spectrum for motor oil which again shows little error in the mid-wavenumber regions. In general, there is good qualitative agreement between the band positions within the two sets of refractive indices. A correction factor for the carbon dioxide contamination appearing in some of the spectra should be used similar to the water correction factor used before the retrieval process.

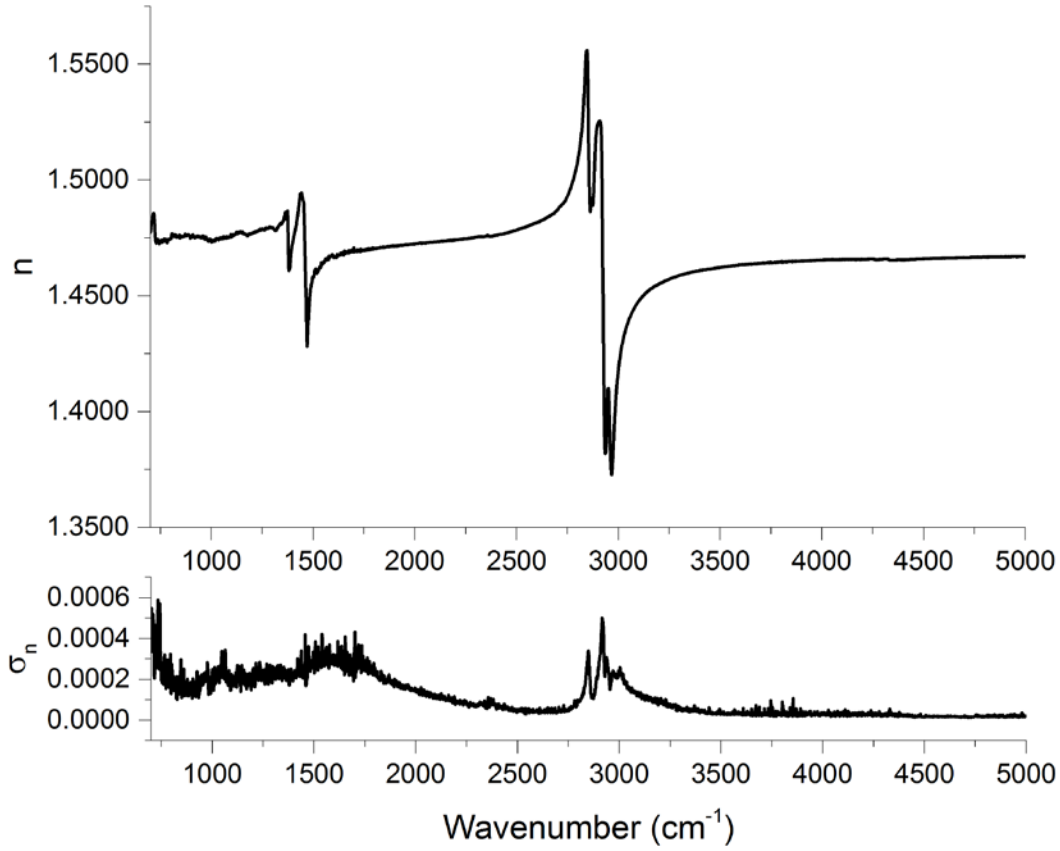

Figure 10: Real Component Spectrum. The top panel provides the real component spectrum for motor oil after subjecting 30 experimental spectra to the Mie retrieval process. The lower panel shows the error associated in the spectrum again with a small peak of approximately 2400 cm^{-1} appearing for CO_2 uncertainty.

From previous work, the imaginary component spectrum for motor oil shares qualities that are similar to squalane (**Figure 11**). Bands for squalane and motor at the 2800-3000 cm^{-1} and 1300-1500 cm^{-1} regions are shared for both aerosol spectra. Squalane, a tetracosane compound, is a common chemical having a substantial concentration in oils such as olive oil, peanut oil and amaranth oil.[6]

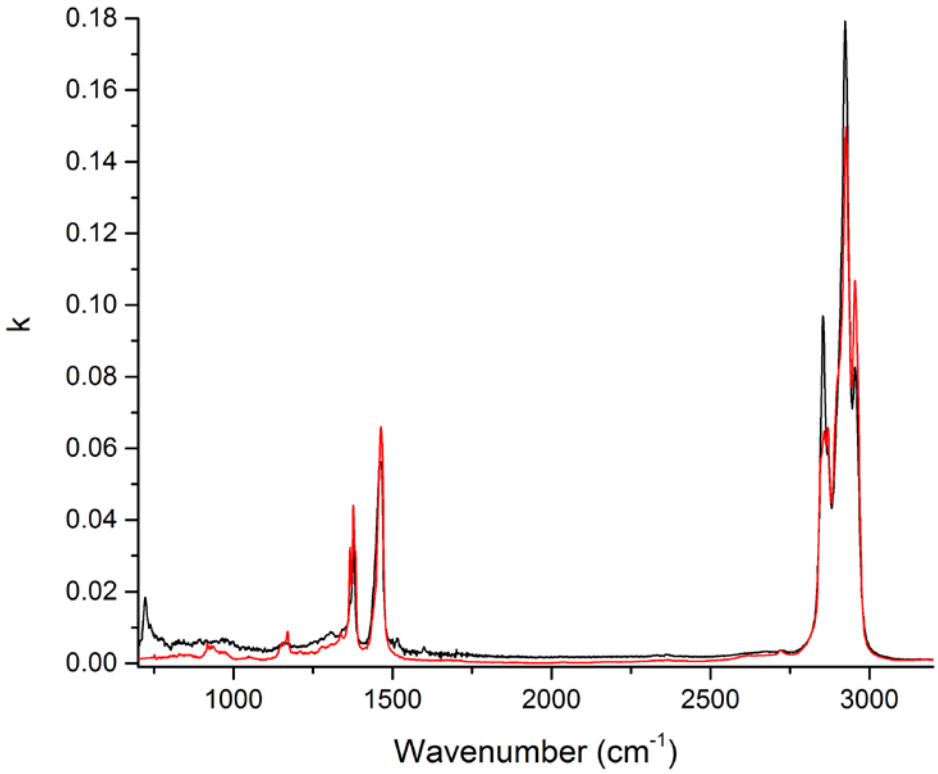

Figure 11: Imaginary Component Spectrum of Motor Oil and Squalane. The above graph provides the imaginary components of motor oil (black line) overlaid with that of squalene (red).

SUMMARY

This study is the first case to successfully retrieve the complex refractive indices for motor oil aerosols. Interestingly, motor oil shares similarities in its absorption features with that of squalane, a tetracosane based hydrocarbon. Still, further analysis needs to be continued in order to minimize the associated complex refractive index set error. One error minimization that will be done is to correct the aerosol spectra for CO_2 contamination. Furthermore, the applicability of the index set must be tested against a greater set of generated motor oil aerosol ensembles. Future work for this project will include testing generated motor aerosol at much higher temperatures than

350 ^{o}C. A decarboxylation reaction seems to be occurring as the motor oil is heated to high temperatures, however the relationship between the two variables is not exactly known. Besides Pennzoil 5w-20, other brands and types of motor oil should be used to better understand differences in complex refractive indices. With more information surrounding motor oil, scientists in the field can better able understand the impact that motor oil aerosols have on the environment.

ACKNOLEDGMENTS

First, I thank my thesis mentor Dr. Richard F. Niedziela for his guidance and patience during these past four years. I thank Dr. Graham Griffin for taking the time to be my faculty reader and to help develop the final thesis product. I thank Stephanie E. Goyette, and Daniel J. Olesak for assisting in the experimental runs and for making the lab an enjoyable work environment. I also would like to thank Myles Edwards for his advice and solutions to problems that had commonly occurred throughout the project. Lastly, I would like to thank Nancy Grossman and the DePaul Honors Department for allowing me to take on this particular science thesis project.

REFERENCES

[1]Harley, R. McKeen, S., Pearson J., Rodgers, M., Lonneman, W., *Analysis of motor vehicle emissions during the Nashville/Middle Tennessee Ozone Study*, Journal of Geophysical Research. **2001,** Pg. 3559-3567.

[2]Bassbasi, M. Hafid, A. Platikanov, S. Tauler, R. Oussama, A., *Study of motor oil adulteration by infrared spectroscopy and chemometrics methods*, Fuel. **2013,** Pg. 798-804.

[3]Zieba-Palus, J. Koscielniak, P., *Differentiation of motor oils by infrared spectroscopy and elemental analysis for criminalistics purposes*, Journal of Molecular Structure. **1999,** Pg. 533-538.

[4] Dohm, M.; Postscavage, A.; Niedziela, R. *Infrared Complex Refractive Indices for Nopinone*. J. Phys. Chem. A, **2004**, Pg. 5365.

[5] McGinty, S.; Kapala, M.; Niedziela, R. *Mid-infrared complex refractive indices for oleic acid and optical properties of model oleic acid/water aerosols*. Phys. Chem. Chem. Phys. **2009**, Pg. 7998-8004.

[6]Allison, A. *Squalene and Squalane Emulsion as Adjuvants*. *Methods.* **1999,** Pg. 87-93.

[7]Koscielniak, P. Zieba-Palus, J. Lacki, M., *Differentiation of used motor oils on the basis of their IR spectra with application of cluster analysis*. Journal of Molecular Structure. **2001,** Pg. 221-228.

[8]Balabin, R. Safieva, R., *Motor oil classification by base stock and viscosity based on near infrared (NIR) spectroscopy data*, Fuel. **2008,** Pg. 2745-2572.

[9]Balabin, R. Safieva, R. Lomakina, E., *Near-infrared (NIR) spectroscopy for motor oil classification: From discrimination analysis to support vector machines*, Microchemical Journal **2011,** Pg. 121-128